DOI: 10.1007/s11099-015-0163-9 PHOTOSYNTHETICA 54 (1): 101-109, 2016

Measurements of reflectance and fluorescence spectra for nondestructive characterizing ripeness of grapevine berries

M. NAVRÁTIL[*,+] and C. BUSCHMANN[**]

Faculty of Science, Department of Physics, University of Ostrava, Chittussiho 10, CZ-710 00 Slezská Ostrava, Czech Republic[*]
Botanical Institute, Karlsruhe Institute of Technology (KIT), Kaiserstr. 12, D-76128 Karlsruhe, Germany[**]

Abstract

In vivo reflectance and fluorescence spectra from berry skins of a white (Riesling) and red (Cabernet Sauvignon) grapevine variety were measured during a ripening season with a new CMOS radiometer instrument. Classical reference measurements were also carried out for a sugar content of the berry juice [°Brix] and pigment contents (chlorophyll *a* and *b*, carotenoids, anthocyanins) from methanol extracts of the berry skin. We showed that the colours and the spectra analysed from them could be taken as an unambiguous indicator of grapevine ripening. Reflectance spectra, which were affected by the content of pigments (chlorophylls and anthocyanins), effects of surface (wax layers), and tissue structure (cell size) of the berries well correlated ($R^2 = 0.89$) with the °Brix measurements of the berries. The fast data acquisition of both reflectance and fluorescence spectra in one sample with our radiometer instrument made it superior over the time-consuming, traditional, and mostly destructive chemical analysis used in vine-growing management.

Additional key words: Cabernet Sauvignon; CIE 1931; plant pigments; Riesling.

Introduction

The knowledge about the process of grapevine ripening is of utmost importance for the production of high quality wines since it allows harvesting selectively berries in right time and at the right location. A high variability in ripening within a vineyard makes difficult to determine when the time of the best possible ripeness comes in a vineyard with a large variation in berry maturity. The berry maturity is not homogeneous even within a grape cluster (Coombe 1987, Coombe and McCarthy 2000). Grapes naturally exhibit a growth curve comprising of three stages. During the first stage, the berry shows rapid cell division, associated with cell enlargement and accumulation of various substances [*e.g.* tannins, hydroxycinnamic acid, minerals, tartaric and malic acid (Romeyer *et al.* 1983, Possner and Kliewer 1985, Kennedy *et al.* 2001)]. The initial phase typically extends between six and eight weeks. The second stage is a transitional period, most variable in duration (1–6 weeks), that largely establishes a cultivar's early or late maturing character. At the end of this stage, the berry begins to lose its green colour and further colour changes of the berry start (Jackson 2008). This turning point, called *véraison*, signifies the beginning of a fundamental physiological shift that culminates in the berry maturation (the stage three). Generally, ripening is associated with enlargement of the berry, tissue softening, a decrease in acidity, the accumulation of sugars, the synthesis of anthocyanins (Anth; in red-skinned varieties), and the acquisition of aroma compounds. The third stage usually lasts about 5–8 weeks (Harris *et al.* 1968, Coombe *et al.* 2000, Jackson 2008).

When young, cells of hypodermis (*i.e.* variable number of tightly packed layers of mesophyll cells) are photosynthetically active. After *véraison*, the plastids lose their chlorophyll (Chl), carotenoid (Car), and starch contents, and begin to accumulate oil droplets (Jackson 2008).

Both the appearance and the interior characteristics are the aspects that can be used as a quality criterion of grapes. The traditional way of characterizing the grape ripeness comprises phenotyping of the size and colour of the developing berries by visual observation. Chemical

Received 8 June 2014, *accepted* 22 June 2015, *published as online-first* 18 July 2015.
[+]Corresponding author; phone: +420 597 09 2155, e-mail: Martin.Navratil@osu.cz
Abbreviations: Anth – anthocyanins; Car – carotenoids; Chl – chlorophyll; NDVI – normalized difference vegetation index.
Acknowledgements: This project was supported by EU, Commission of the European Communities, 7th Framework program FP7-SME-2010-1-262011. The manuscript has been written during the stay of the first author at the Karlsruhe Institute of Technology (KIT) partially financed by the project "BioNetwork" (reg. number: CZ.1.07/2.4.00/31.0025). We would like also to acknowledge the help with measurements and data processing by Philipp Epple, Zishang Jiang, Vanessa Kunz, Marie Opálková, and Gregor Ziegler.

analysis is needed for a more precise detection of accumulation and transformation of acids as well as the production of individual sugars and pigments (*e.g*. Anth). These chemical analyses are not only time-consuming and expensive, but also destructive, *i.e*. a part of the grapes is lost (Cao *et al.* 2010). Only in case of the sugar content, an easy and relatively fast, traditional physical method is applied (refractometer reading of °Brix), but this method is also destructive. Thus, nondestructive testing of properties and characteristics in crops (mainly fruits and vegetables) is critical for monitoring and controlling product quality and safety (Ben Ghozlen *et al.* 2010*,* for a review *see* Ruiz-Altisent *et al.* 2010).

Vis/NIR reflectance and fluorescence spectra can be taken and compared to reference measurements usually carried out during a wine production. From the reflectance spectra, changes of pigment concentrations and many other skin and inner properties can be detected and predicted, *e.g.* soluble solids content and pH of grapes (Cao *et al.* 2010), oranges (Jamshidi *et al.* 2012), apples (Abu-Khalaf and Bennedsen 2004), and many others (for a review *see* also Cozzolino *et al.* 2006). The absorption characteristics of Chls, Car, and Anth (in case of red vine) show their typical bands in the visible part of the reflectance spectrum between 400 and 700 nm (Agati *et al.* 2005*,* Zhang *et al.* 2013*,* for a review *see e.g*. Buschmann *et al*. 2012). Colours deduced from these reflectance spectra can be used to specify the visual impression (Malacara 2002) independent of an observer and irradiation, which is changing with sun angle and weather condition. Colour characteristics are often used for description and monitoring of various parameters of seeds (*e.g*. Granitto *et al.* 2002*,* 2005*,* Mebatsion *et al.* 2013), fruits (*e.g*. Kondo *et al.* 2000*,* Kurtulmus *et al.* 2011*,* Mollazade *et al.* 2012*,* Rodríguez-Pulido *et al.* 2012*,* Payne *et al.* 2013), leaves (*e.g*. Buschmann and Nagel 1993*,* Buschmann *et al.* 2012) or entire plants or vegetation (*e.g*. Onyango and Marchant 2003*,* Meyer *et al.* 2004). From fluorescence spectra, characteristics of Chl molecules can be deduced (Papageorgiou and Govinjee 2004). The fluorescence is highly specific (Valeur and Berberan-Santos 2012) since only Chl *a* is the pigment emitting red fluorescence upon irradiation with blue light in intact plant material. A decline of the Chl content during ripening of white grape berries has been monitored noninvasively by recording intensities of Chl fluorescence excited by visible radiation (Kolb *et al.* 2006*,* Lenk *et al.* 2007). The authors showed that Chl fluorescence intensity declined in parallel with increasing sugar contents, which proved that Chl degradation was a part of the global ripening process in grape berries under natural conditions.

Most of the knowledge on reflectance and fluorescence in intact plant materials is based on leaf measurements since these optical measurements are the basis for agricultural and environmental quality control from close distance to remote sensing (Jones and Vaugham 2010, Tremblay *et al*. 2012). Although there is a difference in tissue structure between leaves and berry skins (Jackson 2008), the majority of the essential parameters is similar because pigments are located in the same cell organelles. In particular, the presence of intercellular spaces has a significant influence on the physical properties of tissues, which vary with the size of these spaces during ripening (Pieczywek and Zdunek 2012). Chl and Car are always found as pigment-protein complexes in the internal chloroplast membranes (thylakoids) (*e.g*. Buschmann and Nagel 1993), while Anth are always dissolved in the vacuole of the plant cell.

Here, we presented a part of our extensive study carried out in 2012 with grapevine of Riesling (white vine) and Cabernet Sauvignon (red vine) variety.

Materials and methods

Plant material: The grapes were taken from the vineyards of the Julius Kühn Institute for Grapevine Breeding "Geilweilerhof" (N 49°13.048', E 008°02.752') at Siebeldingen, which belongs to the official German wine region "Palatinate" (Pfalz). We investigated berries from grapevine (*Vitis vinifera* L.) cultivars that are used in white (cv. Riesling) and red (cv. Cabernet Sauvignon) wine production. The vines were planted in 2000. Grape clusters were collected weekly from 13 August until the end of ripening season (end of September 2012). In the vineyard, two clusters of each variety were stored in dark and humid conditions at 4°C, then transferred to the laboratory at Karlsruhe Institute of Technology where they were immediately analysed or kept overnight at 4°C until analysis.

Sample preparation: Eight individual berries were taken from the middle part of two clusters of both Riesling and Cabernet Sauvignon varieties. The berries were chosen as being representative for the colour of the entire cluster. First, fluorescence and reflectance spectra were measured. After spectral measurements, the berries were imaged by means of a flat-bed scanner (*Epson Perfection 3200 Photo, Epson,* Meerbusch, Germany). Colour images were taken with a resolution of 300 dpi. Colour coordinates from the scanner images were analysed by an open-source software (*CIEWI, The Wavelength Picker, Version 03.03.00* www.eickholz.de/ciewi). Since a scanner uses its own internal calibration using always the same preheated light source, further calibration is not needed for comparison measurements. Further, the projection area (*i.e*. berry size) as well as colour coordinates were obtained from these images. Subsequently, the berries were cut in two halves and the sugar content in °Brix (1 °Brix represents 1 g of sucrose in 100 g of solution) was measured by squeezing a drop of the juice on a hand-held refractometer (*VWN3,*

KEBA, Breisach, Germany). After that, pigment analysis was performed.

Spectral measurements: Fluorescence and reflectance spectra were acquired using a hand-held spectrophotometer (modified version of *SpectraPen, PSI,* Brno, Czech Republic) equipped with internal light sources capable of measuring both reflectance and fluorescence in the spectral range of 325–790 nm. The following light sources were used: incandescent xenon lamp (emission from 380 to 1050 nm) for reflectance measurements and blue LED with maximum at about 450 nm for fluorescence measurements. Signal detection is achieved by a compact polychromator integrated with a reflection grating and CMOS linear image sensor *S8378-256Q* (*Hamamatsu*, Herrsching am Ammersee, Germany) with the spectral resolution (full width at half maximum) of 9 nm. For calibration of reflectance measurements, grey reflectance standards with 5 and 20% reflectance (*Zenith, SphereOptics* Uhldingen, Germany), respectively, were used. No further correction was carried out.

From the reflectance spectra, we determined colour coordinates: RGB values as well as x and y coordinates, brightness, and dominating wavelength according to CIE 1931. The colour coordinates calculated from the reflectance spectra measured with our instrument more strongly correlated (in area and illumination source) with the reflectance parameters than those from the flat-bed scanner. Correlations of data from the reflectance spectra (*e.g*. le Maire *et al.* 2004) were carried out with the sugar content and pigment analysis. Reflectance data were acquired at 1.8 nm interval and three neighboring data were averaged in order to exclude fluctuation of the data based on signal noise.

Pigment analysis: For the quantitative analysis of Chl *a* and Chl *b* as well as of total Car, we always used an exposed part of the berry, *i.e*. we made a mark (circle using marker) on the berry skin in the field to know later which part of the berry was mostly faced to light. From this part, a circular skin area with a diameter of 8 mm was cut by means of a cork borer and the grape flesh was scrapped off with a razor blade. The skin was transferred into a 2 ml Eppendorf tube and homogenized together with 1.5 ml of 100% methanol and a small amount of quartz sand using a micropestle. The homogenized extract was then centrifuged (*Varifuge RF, Heraeus Sepatech,* Osterode, Germany) at 2000 x g for 8 min at 4°C. From the nonturbid transparent supernatant, an aliquot of 1 ml was transferred into a microcuvette (*Hellma Analytics*, Müllheim, Germany). Finally, the absorbance of the extract was measured by a spectrometer (*Specord 210, Analytik Jena*, Jena, Germany) between 200 and 800 nm. The concentrations of the pigments were determined using equations of Lichtenthaler (1987). To the red vine berries, 0.067 ml of HCl was subsequently added. The concentration of 0.1% (w/v) HCl converted all Anth into its visible form (Steele *et al*. (2009); other photosynthetic pigments were entirely destroyed and the absorbance spectrum was determined again. The Anth concentration was quantified using an absorption coefficient of 30 mM^{-1} cm^{-1} at 530 nm. The pigment content was expressed in μg [malvidin unit] m^{-2} of the berry area (Steele *et al.* 2009). The molecular mass for malvidin is 331 (Tian *et al*. 2005).

Software used for data processing and statistical analysis: Data processing was carried out using a spreadsheet program (*Microsoft Excel 2010*). The reflectance spectra in the visible range (between 400 and 700 nm) were used to determine the colour in two systems: (*1*) RGB colour model (maximum at 640 nm, 550 nm, and 460 nm for red, green, and blue, respectively) and (*2*) CIE 1931 colour space (using the colour matching functions for the CIE standard daylight illuminant D65). For the determination of the projected berry area, graphics software was used (*Adobe Photoshop CS v.8.0.1*). Averages of each parameter were analysed using the *Student*'s *t*-test to compare selected values.

Results

Calculation of the berry projection area revealed an increase during the vegetation period from 130 to *ca*. 200 mm^2 in both vine varieties. The fastest changes occurred when the production of sugars started (second third of August, part of the season called *véraison*) (Table 1). The sugar content of single berries was very low (°Brix below 5°, Table 1) at the beginning of our measuring period, but the fast increase followed starting from 20 August. During the rest of the ripening period, the sugar content of both white and red variety rose and reached the maximum of *ca*. 20 and 22 °Brix for white and red vine, respectively, during the week of harvest. After that, the sugar content did not change (data not shown). The sugar content of the Riesling berries was always lower than that of Cabernet Sauvignon (by *ca*. 10–20%); the differences were always statistically significant except for the first measuring day (Table 1).

Standard analysis of photosynthetically active pigments and their ratios in berry skin confirmed the expected decrease of the Chl (*a*+*b*) content and relatively stable content of total Car during the ripening process except the second measuring week, when Car dropped significantly from 27 to 17 mg m^{-2} in Cabernet Sauvignon (Table 2). The content of Chl *b* was more stable in the red variety from the middle to the end of the season contrary to the white one, where it was opposite. The absolute

Table 1. Comparison of single berry projection area and the sugar content of single berries determined with a refractometer for white (Riesling) and red (Cabernet Sauvignon) variety during the ripening season. Changes in the content of anthocyanins in the red variety during the ripening season as detected from the absorption spectra of methanol extracts after addition of HCl (0.1 %). Averages and SD for $n = 8$ are presented. For anthocyanins and projection area, the statistical differences between subsequent days of measurement are presented by *, **, which indicates significant effects at 0.05 and 0.01 levels, respectively. ns – not significant. For sugar content, statistical differences between both varieties for the same measuring day were tested.

Variety	Day	Projection area [mm^2]	Sugar content [°Brix]	Anthocyanins [μg m^{-2}]
Riesling	Aug 13	132.67 ± 6.99^{ns}	4.63 ± 0.43^{ns}	
	Aug 20	133.91 ± 8.84**	6.06 ± 1.61**	
	Aug 27	151.60 ± 11.58^{ns}	11.40 ± 2.24**	
	Sept 03	142.49 ± 7.99**	11.73 ± 3.49**	
	Sept 17	186.31 ± 19.10^{ns}	17.33 ± 0.82**	
	Oct 01	182.44 ± 13.42	19.95 ± 1.24*	
Cabernet	Aug 13	125.34 ± 8.09^{ns}	4.71 ± 0.25	0.06 ± 0.01**
Sauvignon	Aug 20	127.57 ± 6.27*	10.10 ± 0.58	1.00 ± 0.69**
	Aug 27	141.04 ± 14.43*	14.53 ± 0.56	5.40 ± 1.37**
	Sept 03	163.31 ± 18.72^{ns}	15.56 ± 0.92	8.25 ± 2.11*
	Sept 17	155.81 ± 12.46^{ns}	19.01 ± 0.58	11.19 ± 1.84^{ns}
	Oct 01	172.64 ± 27.20	21.24 ± 1.05	11.68 ± 2.68

Table 2. Content of photosynthetically active pigments and their ratios in berries of white (Riesling) and red (Cabernet Sauvignon) variety. Chlorophyll (Chl) *a*, Chl *b*, and total carotenoids (Car) were detected from the absorption spectra of methanol extracts. Averages and SD for $n = 8$ are presented. The statistical differences between subsequent days of measurement are presented by *, **, which indicates significant effects at 0.05 and 0.01 levels, respectively. ns – not significant.

Variety	Day	Chl *a* [mg m^{-2}]	Chl *b* [mg m^{-2}]	Car [mg m^{-2}]	Chl (*a*+*b*) [mg m^{-2}]	Chl *a*/*b*	Chl (*a*+*b*)/Car
Riesling	Aug 13	54.22 ± 10.99^{ns}	20.06 ± 2.71^{ns}	19.25 ± 2.96^{ns}	74.28 ± 13.37^{ns}	2.69 ± 0.34^{ns}	3.85 ± 0.24^{ns}
	Aug 20	51.52 ± 10.24^{ns}	19.77 ± 4.49^{ns}	17.43 ± 4.81^{ns}	71.29 ± 14.58^{ns}	2.63 ± 0.22*	4.16 ± 0.39**
	Aug 27	50.75 ± 11.41^{ns}	17.17 ± 3.37^{ns}	19.72 ± 4.38^{ns}	67.93 ± 14.57^{ns}	2.95 ± 0.27^{ns}	3.48 ± 0.41^{ns}
	Sept 03	46.12 ± 13.70**	16.29 ± 4.62**	19.44 ± 4.39*	62.48 ± 18.29**	2.83 ± 0.12^{ns}	3.19 ± 0.36**
	Sept 17	28.47 ± 3.58^{ns}	10.86 ± 1.91^{ns}	15.34 ± 2.41^{ns}	39.33 ± 5.10^{ns}	2.66 ± 0.36^{ns}	2.59 ± 0.31^{ns}
	Oct 01	27.84 ± 4.70	9.14 ± 1.67	15.82 ± 1.67	36.98 ± 5.86	3.09 ± 0.51	2.36 ± 0.45
Cabernet	Aug 13	81.09 ± 7.82**	27.36 ± 2.48**	27.82 ± 2.36**	108.45 ± 9.29**	2.98 ± 0.29*	3.92 ± 0.41^{ns}
Sauvignon	Aug 20	45.72 ± 5.37**	16.99 ± 2.39*	17.06 ± 3.23^{ns}	62.71 ± 7.57^{ns}	2.70 ± 0.17**	3.73 ± 0.43**
	Aug 27	37.25 ± 4.34^{ns}	20.12 ± 2.28*	20.89 ± 4.10^{ns}	57.37 ± 5.00^{ns}	1.87 ± 0.29^{ns}	2.82 ± 0.51^{ns}
	Sept 03	36.35 ± 4.92**	23.72 ± 2.98^{ns}	19.43 ± 2.35^{ns}	60.07 ± 4.74**	1.56 ± 0.33^{ns}	3.12 ± 0.31**
	Sept 17	29.15 ± 1.97*	22.50 ± 3.29^{ns}	21.25 ± 2.62^{ns}	51.65 ± 5.21^{ns}	1.31 ± 0.12*	2.46 ± 0.37^{ns}
	Oct 01	23.65 ± 5.81	23.81 ± 4.82	19.80 ± 3.78	47.46 ± 7.39	1.03 ± 0.34	2.43 ± 0.37

amount in Cabernet Sauvignon at the beginning of the measuring period was only one third of the amount of Chl *a*; later on, the values of both Chl *a* and Chl *b* were comparable and this resulted in the decrease of Chl *a/b* ratio during the time. Both red and white variety showed degradation to less than one half of their total Chl later on (comparing 13 August and 1 October) (Table 2).

The content of Anth was measured only for the red variety Cabernet Sauvignon. Results showed a strong increase during the ripening season (Table 1). The main changes occurred during the first two weeks of measurement (*ca*. 5.5 times higher content of Anth on 27 August as compared to 20 August) when the berries started to change their colour from green to red and dark blue later on.

Red berries showed a reflectance spectrum without maximum in the green spectral region (with the exception of the first developmental stage). Both white and red berries showed a decrease in the reflectance spectra during the ripening process, most pronounced in the red region (Fig. 1). The most pronounced changes occurred in the red and far-red region and, in the case of Cabernet Sauvignon, in the blue-green spectral region during turning berry colour from green to red and finally to dark blue. The reflectance spectra of both white and red berries were somewhat lower than we could expect from the green-leaf spectra (data not shown) but with a higher "baseline". Further, the red vine variety showed generally the lower reflectance with the minimum of 25% as compared to 35% for white berries.

Fluorescence spectra of both white and red berries recorded in the red spectral region (Chl *a* fluorescence)

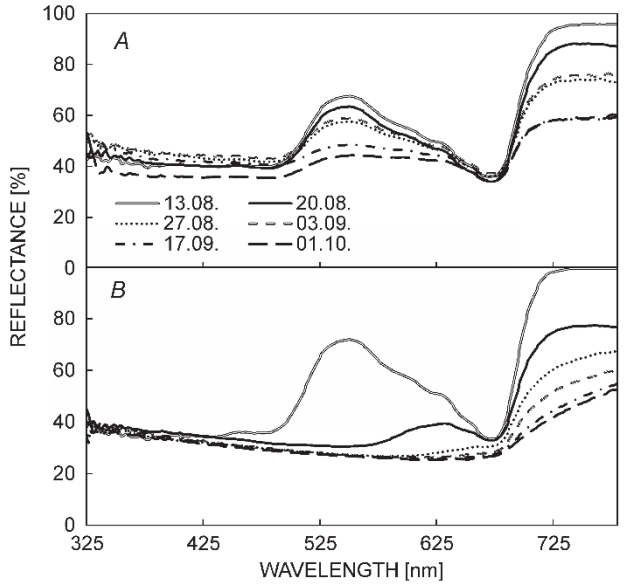

Fig. 1. Reflectance spectra from berries of white (Riesling; *A*) and red (Cabernet Sauvignon; *B*) variety during the ripening process. Averages for $n = 8$ are presented. The differences among individual spectra during one measuring day were less than 10% at the maximum.

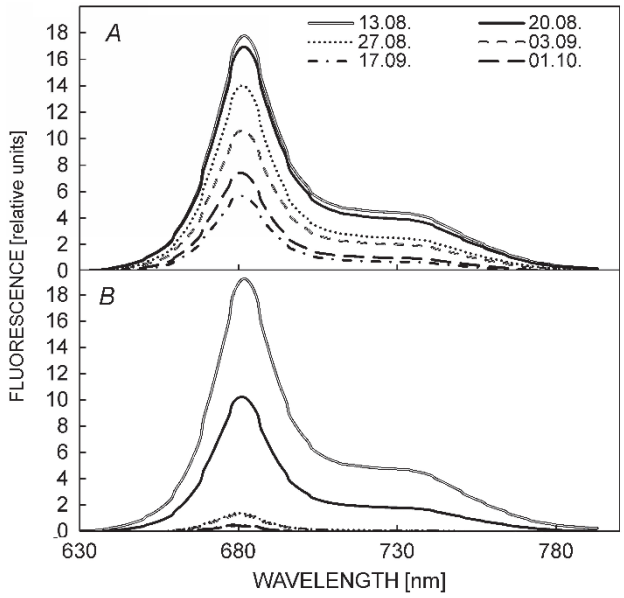

Fig. 2. Fluorescence spectra from berries of white (Riesling; *A*) and red (Cabernet Sauvignon; *B*) variety during the ripening process. Averages for $n = 8$ are presented. The differences among individual spectra during one measuring day were less than 10% at the maximum.

with blue excitation showed a decrease in their intensity (both in the F_{680} and F_{735} maxima) during the ripening process (Fig. 2). At the beginning of our measurements, fluorescence intensity was comparable for white and red variety, but after two weeks (starting at 27 August), the fluorescence spectra obtained for red berries decreased drastically as compared to white berries (reaching then only *ca*. 10% of white berries values). In the case of the red berries, the main changes in F_{680}/F_{735} ratio occurred during the first two weeks of berry development and this ratio was rather stable later on. On the other hand, the white berries showed a gradual increase from 4 at the beginning to 7.3 at the end (Fig. 3).

The RGB values obtained from the reflectance spectra showed higher differences between the three colour channels for the red variety during the first two weeks of our measurements and remained stable later on. On the other hand, the white vine berries were continuously changing their colour during the ripening season which resulted in a slow but continual decrease in the green channel and also in a significant difference in the blue channel between 13 August and 1 October (Fig. 4). CIE x and y coordinates of the red variety followed a pattern similar to the RGB values with higher differences at the beginning and negligible changes afterwards. CIE coordinates of the white vine berries were slightly higher and showed a gradual decrease during the time as compared to the red ones. The x coordinate of the white variety was (except at the very beginning) always higher (from *ca*. 7% on 20 August to 10% on 1 October) comparing to the red variety (Fig. 5).

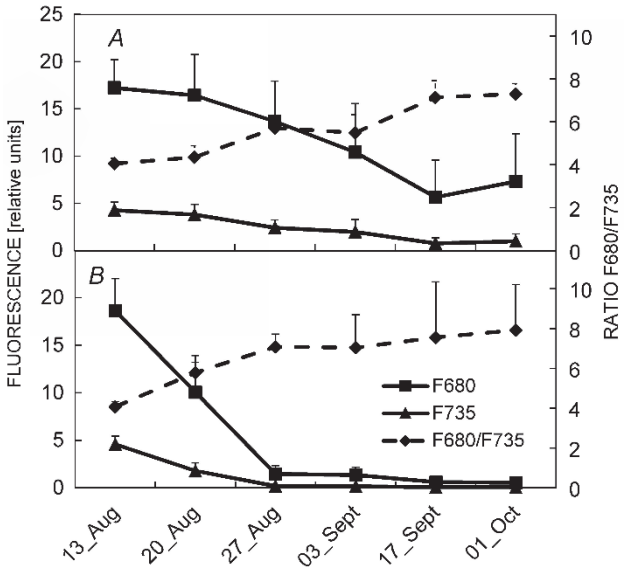

Fig. 3. Fluorescence intensity in the maximum at 680 nm (F680) and 735 nm (F735) and the fluorescence ratio F680/F735 of berries of white (Riesling; *A*) and red (Cabernet Sauvignon; *B*) variety during the ripening process. Averages and SD for $n = 8$ are presented.

The time development of the dominating wavelength showed that at the beginning both the white and red vine varieties had the same colour with the dominating wavelength in the green at *ca*. 560 nm. After the beginning of sugar production, *i.e*. onset of *véraison* on 20 August,

the red variety changed its dominating wavelength to a value close to 480 nm, which corresponds to a blue colour, and after that, the values were stable until the harvest (Fig. 5). White vine berries changed their colour in the range of different grades of green and finally became green-brown during the harvest week.

At the beginning of their development, brightness was similar for both white and red berries, but after the significant colour change of red vine, its brightness decreased to one half of the white vine values and remained the same until the harvest. On the other hand, the white variety showed a slight decrease during the time.

Colour saturation of the white variety started at 15% and gradually decreased to 5% at the end of the season. The red variety started at 23% and dropped to less than 10% after the first week of development, while remained stable later on (Fig. 5).

Linear correlation of optical characteristics [represented by reflectance parameter $(R_{750} - R_{680})/(R_{750} + R_{680})$ and two different "chemical" characteristics] revealed a very good relationship between the reflectance and sugar content (coefficient of determination R^2 higher than 0.85 in both varieties) and a good correlation of reflectance and the total Chl content expressed per berry skin area (R^2 = 0.68 and 0.71 for the white or red variety, respectively) (Fig. 6). The main changes occurred between 13 and 20 August (time of *véraison*) with only slight changes later on. This was the characteristic especially of the red variety; Chl were degraded together with hiding of the green colour behind Anth.

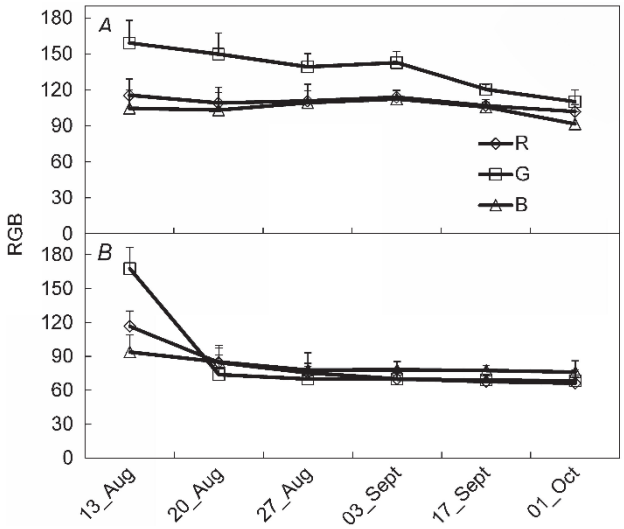

Fig. 4. Colour analysis of berries of the white (Riesling; *A*) and red (Cabernet Sauvignon; *B*) vine variety during the ripening process. Red (R), green (G), and blue (B) channels were calculated from reflectance spectra. Averages and SD for n = 8 are presented.

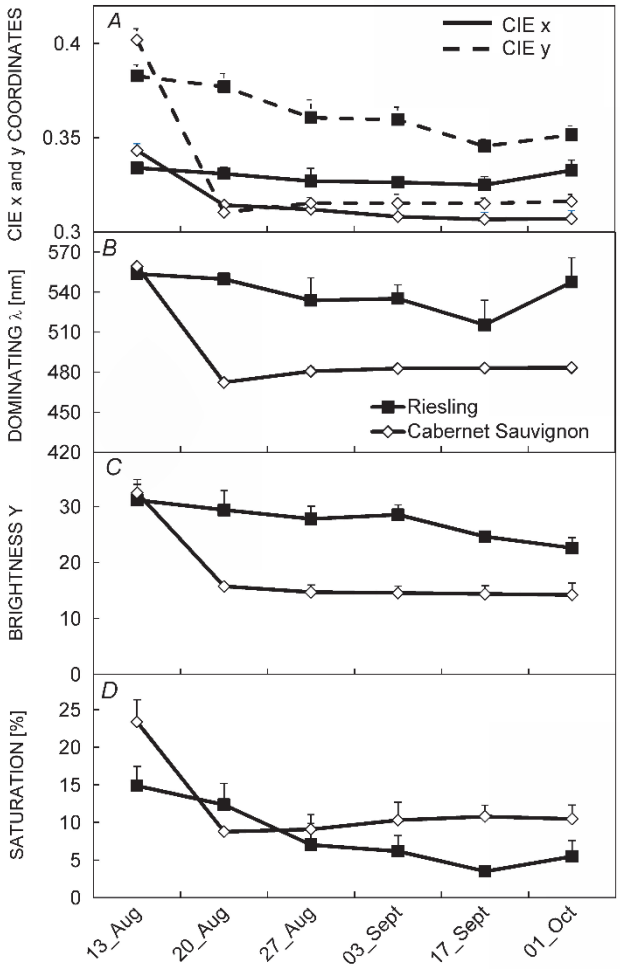

Fig. 5. Colour analysis of berries of the white (Riesling) and red (Cabernet Sauvignon) vine variety during the ripening process. CIE x and y coordinates (*A*), dominating wavelength (*B*), brightness Y (*C*), and colour saturation (*D*) were calculated from reflectance spectra. Averages and SD for n = 8 are presented.

Discussion

Most pigments as well as flavor and taste determining compounds are located in the berry skin (Coombe 1987) that makes it the most important part for later quality of the wine production. *In vivo* reflectance and fluorescence spectra of berries are determined by the properties of the berry skin. Both optical detection techniques applied here in contact measurements are also used for remote sensing of vegetation (Jones and Vaugham 2010). The reflectance spectra in the range between 325 and 790 nm (*i.e.* from UV-A *via* visible radiation to the near infrared) are influenced by the absorption of Chls, Car, flavonoids, and Anth which reduces the reflectance in their specific bands.

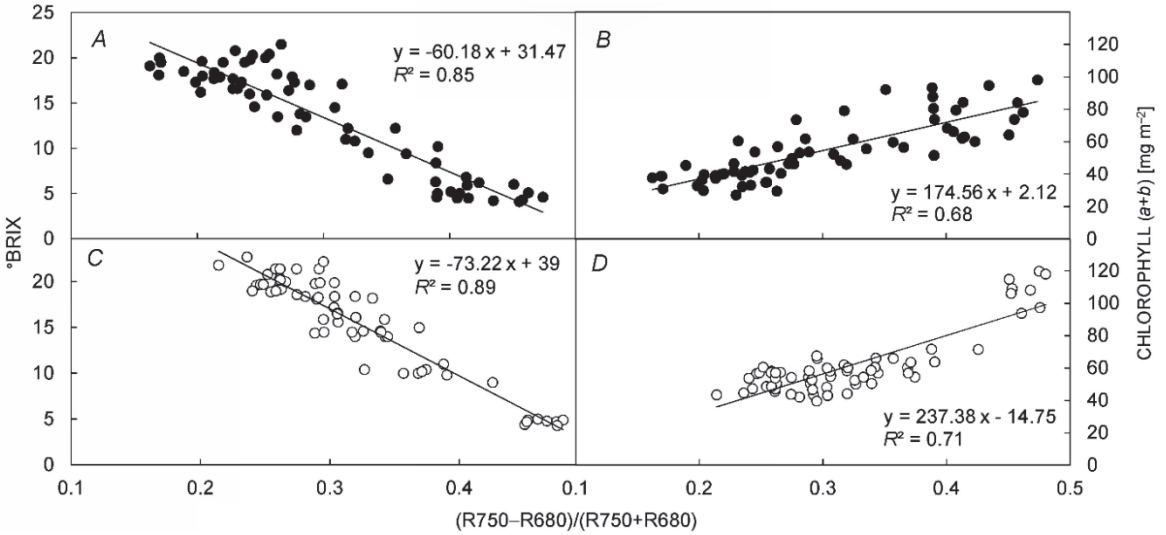

Fig. 6. Linear correlations of the reflectance index [$(R_{750}–R_{680})/(R_{750}+R_{680})$] and sugar content expressed in °Brix and total chlorophyll content expressed in mg m^{-2} for the white (Riesling; *A*,*B*) and red (Cabernet Sauvignon; *C*,*D*) variety. Coefficients of determination R^2 together with the equation of the regression line are presented. Number of samples $n = 64$.

Waxes at the surface of the berry skin lead to a homogeneously increased reflectance over the entire spectral range, while the size of cells as well as the aerial interspaces in tissues affect the scattering in the near infrared range (Buschmann *et al.* 2012). The shape of our spectra was similar to results obtained by other authors (Rustioni *et al.* 2013, 2014), but the slight increase in reflectance from green towards UV and very high reflectance in the near infrared was obviously caused by the technical set-up of our instrument (particularly, use of two grey standards and characteristics of the detector).

The reflectance parameter $(R_{750} – R_{680})/(R_{750} + R_{680})$, which was shown to have a good linear correlation with °Brix and the Chl content of the berry skin of the white and red variety (Fig. 6), resembles the widely used normalized difference vegetation index [NDVI: $(R_{800} – R_{680})/(R_{800} + R_{680})$, Rouse *et al.* (1974)]. However, the NDVI is originally based on the assumption that it represents the Chl absorption which is sensed as reduced reflectance at 680 nm taking the reflectance at 800 nm as a constant reference. As it can be seen from the reflectance spectra (Fig. 1), in case of grapevine berries, it is rather the long-wavelength reflectance at 750 nm than the reflectance at 680 nm which changes during ripening. Thus, the Chl absorption represented in the reflectance at 680 nm is rather constant whereas the decrease at 750 nm can be attributed to the increasing cell size during ripening in the phase three (during *véraison*). The good linear correlation of the parameter $(R_{750} – R_{680})/(R_{750} + R_{680})$ with the °Brix occurred not due to the sugar content but due to the cell size changes that went along with the berry ripening. The increase of the berry size (Table 1) at the last part of the ripening process occurred mainly due to the increase of the cell size of the berry skin rather than an increase of a cell number (Coombe and McCarthy 2000, Jackson 2008). In our case, NDVI showed always worse correlation than that of the ratio of $(R_{750} – R_{680})/ (R_{750} + R_{680})$ (data not shown).

The strong decrease of the reflectance in the 550 nm range (green light) observed in the reflectance data of the red variety (Fig. 1) was not due to the increased Chl but rather due to the formation of Anth (Table 1); it is characterized by a maximum absorption in the green (Agati *et al.* 2005, Rustioni *et al.* 2014) and even a relatively low amount of Anth is sufficient to reduce the reflectance at the green region (Rustioni *et al.* 2014). The strong accumulation of Anth also leads to the decrease of brightness (CIE parameter Y) and the shift of the dominating wavelength from green (550 nm) to blue (480 nm) (Fig. 5). The loss in brightness could be also seen from the strong decrease of the RGB values (Fig. 4).

The colour analysis carried out with the reflectance spectra in the visible range (400 to 700 nm) represents an unambiguous definition of the visible impression, which is independent of the current radiation (sunlight, clouds, daytime) and eye of an observer (Malacara 2002). For this analysis, the entire spectrum is needed; it is given by the CMOS radiometer in contrast to other instruments, which determine only a limited number of bands. One can clearly identify the colour change during ripening and the difference between the white and red variety.

The fluorescence spectra between 650 and 800 nm (Fig. 2) showed the same shape as those known for green leaves (*e.g.* Buschmann 2007), grapes (Agati *et al.* 2007), and olives (Agati *et al.* 2005). In contrast to reflectance signals, which are influenced by many compounds, the fluorescence signal is highly specific because it is restricted to only few fluorescence dyes (Valeur and Berberan-Santos 2012). Chl *a* is the dye compound of leaves and berries with fluorescence in the range between 650 and 800 nm (Papageorgiou and Govindjee 2004). The

Chl fluorescence decreased during the ripening process. This strong decrease cannot be attributed only to the decrease of the Chl content in case of Cabernet Sauvignon since it was much stronger for the red variety than that for the white variety. The fluorescence can be reduced by the penetration of the excitation light (Buschmann 2007) that is hindered for the red variety due to the accumulation of Anth (Agati *et al.* 2005). In case of Riesling, the decrease of Chl fluorescence (Fig. 3) might be due to the decrease of the Chl content per area of the berry skin. The ratio between the two emission maxima at 680 and 735 nm shows an increase during ripening which is representative for the decrease of Chl per area (Buschmann 2007) and which could be observed also from the extracts data for the Chl analysis of the berry skin (Table 2).

Further correlation models could take advantage of the parallel measurement of entire reflectance and fluorescence spectra. This could help in finding the best harvest time, selecting top-quality grapes, and eliminating unripe or quality reducing fruits. Many fast nondestructive measurements carried out with geo-location data uploaded to a central server may create quality maps of a vineyard. The latest advantages of correlation models can be rapidly implemented in this central server.

References

Abu-Khalaf N., Bennedsen B.S.: Near infrared (NIR) technology and multivariate data analysis for sensing taste attributes of apples. – Int. Agrophys. **18**: 203-211, 2004.

Agati G., Pinelli P., Ebner S.C. *et al*.: Nondestructive evaluation of anthocyanins in olive (*Olea europaea*) fruits by *in situ* chlorophyll fluorescence spectroscopy. – J. Agr. Food Chem. **53**: 1354-1363, 2005.

Agati G., Meyer S., Matteini P., Cerovic Z.G.: Assessment of anthocyanins in grape (*Vitis vinifera* L.) berries using a noninvasive chlorophyll fluorescence method. – J. Agr. Food Chem. **55**: 1053-1061, 2007.

Ben Ghozlen N., Cerovic Z.G., Germain C. *et al*.: Non-destructive optical monitoring of grape maturation by proximal sensing. – Sensors **10**: 10040-10068, 2010.

Buschmann C.: Variability and application of the chlorophyll fluorescence emission ratio red/far-red of leaves. – Photosynth. Res. **92**: 261-271, 2007.

Buschmann C., Nagel E.: *In vivo* spectroscopy and internal optics of leaves as basis for remote sensing of vegetation. – Int. J. Remote Sens. **14**: 711-722, 1993.

Buschmann C., Lenk S., Lichtenthaler H.K.: Reflectance spectra and images of green leaves with different tissue structure and chlorophyll content. – Isr. J. Plant Sci. **60**: 49-64, 2012.

Cao F., Wu D., He Y.: Soluble solids content and pH prediction and varieties discrimination of grapes based on visible–near infrared spectroscopy. – Comput. Electron. Agr. **71S**: S15-S18, 2010.

Coombe B.G.: Distribution of solutes within the developing grape berry in relation to its morphology. – Am. J. Enol. Viticult. **38**: 120-127, 1987.

Coombe B.G., McCarthy M.G.: Dynamics of grape berry growth and physiology of ripening. – Aust. J. Grape Wine R. **6**: 131-135, 2000.

Cozzolino D., Dambergs R.G., Janik L. *et al*.: Analysis of grapes and wine by near infrared spectroscopy. – J. Near Infrared Spec. **14**: 279-289, 2006.

Granitto P.M., Navone H.D., Verdes P.F., Ceccatto H.A.: Weed seeds identification by machine vision. – Comput. Electron. Agr. **33**: 91-103, 2002.

Granitto P.M., Verdes P.F., Ceccatto H.A.: Large-scale investigation of weed seed identification by machine vision. – Comput. Electron. Agr. **47**: 15-24, 2005.

Harris J.M., Kriedemann P.E., Possingham J.V.: Anatomical aspects of grape berry development. – Vitis **7**: 106-119, 1968.

Jackson R.S.: Wine Science. Principles and Applications, 3rd ed. Pp. 776. Elsevier, Amsterdam 2008.

Jamshidi B., Minaei S., Mohajerani E., Ghassemian H.: Reflectance Vis/NIR spectroscopy for nondestructive taste characterization of Valencia oranges. – Comput. Electron. Agr. **85**: 64-69, 2012.

Jones H.G., Vaugham R.A.: Remote Sensing of Vegetation. – Principles, Techniques and Applications. Pp. 400. Oxford University Press, Oxford, 2010.

Kennedy J.A., Hayasaka Y., Vidal S. *et al*.: Composition of grape skin proanthocyanidins at different stages of berry development. – J. Agr. Food Chem. **49**: 5348-5355, 2001.

Kolb C.A., Wirth E., Kaiser W.M. *et al*.: Non-invasive evaluation of the degree of ripeness in grape berries (*Vitis vinifera* L. cv. Bacchus and Silvaner) by chlorophyll fluorescence. – J. Agr. Food Chem. **54**: 299-305, 2006.

Kondo N., Ahmad U., Monta M., Murase H.: Machine vision based quality evaluation of *Iyokan* orange fruit using neural networks. – Comput. Electron. Agr. **29**: 135-147, 2000.

Kurtulmus F., Lee W.S., Vardar A.: Green citrus detection using 'eigenfruit', color and circular Gabor texture features under natural outdoor conditions. – Comput. Electron. Agr. **78**: 140-149, 2011.

le Maire G., François C., Dufrêne E.: Towards universal broad leaf chlorophyll indices using PROSPECT simulated database and hyperspectral reflectance measurements. – Remote Sens. Environ. **89**: 1-28, 2004.

Lenk S., Buschmann C., Pfündel E.: *In vivo* assessing flavonols in white grape berries (*Vitis vinifera* L. cv. Pinot Blanc) of different degrees of ripeness using chlorophyll fluorescence imaging. – Funct. Plant Biol. **34**: 1092-1104, 2007.

Lichtenthaler H.K.: Chlorophylls and carotenoids, the pigments of photosynthetic biomembranes. – Methods Enzymol. **148**: 350-382, 1987.

Malacara D.: Color Vision and Colorimetry: Theory and Applications. Pp. 176. SPIE Press, Bellingham 2002.

Mebatsion H.K., Paliwal J., Jayas D.S.: Automatic classification of non-touching cereal grains in digital images using limited morphological and color features. – Comput. Electron. Agr. **90**: 99-105, 2013.

Meyer G.E., Neto J.C., Jones D.D., Hindman T.W.: Intensified fuzzy clusters for classifying plant, soil, and residue regions of interest from color images. – Comput. Electron. Agr. **42**: 161-180, 2004.

Mollazade K., Omid M., Arefi A.: Comparing data mining classifiers for grading raisins based on visual features. – Comput. Electron. Agr. **84**: 124-131, 2012.

Onyango C.M., Marchant J.A.: Segmentation of row crop plants

from weeds using colour and morphology. – Comput. Electron. Agr. **39:** 141-155, 2003.

Papageorgiou G.C., Govindjee: Chlorophyll *a* Fluorescence: A Signature of Photosynthesis. Pp. 820. Springer, Dordrecht 2004.

Payne A.B., Walsh K.B., Subedi P.P., Jarvis D.: Estimation of mango crop yield using image analysis – Segmentation method. – Comput. Electron. Agr. **91**: 57-64, 2013.

Pieczywek P.M., Zdunek A.: Automatic classification of cells and intercellular spaces of apple tissue. – Comput. Electron. Agr. **81:** 72-78, 2012.

Possner D.R.E., Kliewer W.M.: The localization of acids, sugars, potassium and calcium in developing grape berries. – Vitis **24**: 229-240, 1985.

Rodríguez-Pulido F.J., Gómez-Robledo L., Melgosa M. *et al*.: Ripeness estimation of grape berries and seeds by image analysis. – Comput. Electron. Agr. **82**: 128-133, 2012.

Romeyer F.M., Macheix J.J., Goiffon J.P. *et al*.: The browning capacity of grapes. 3. Changes and importance of hydroxycinnamic acid-tartaric acid esters during development and maturation of the fruit." – J. Agr. Food Chem. **31**: 346-349, 1983.

Rouse J.W.J., Haas H.R., Schell A.J., Deering W.D.: Monitoring vegetation systems in the Great Plains with ERTS. – In: Freden S.C., Mercanti E.P., Becker M.A. (ed.): 3rd Earth Resources Technology Satellite-1 Symposium, Volume I: Technical Presentations. NASA SP-351. Pp. 309-317, NASA, Washington, D.C. 1974.

Ruiz-Altisent M., Ruiz-Garcia L., Moreda G.P. *et al*.: Sensors for product characterization and quality of specialty crops – A review. – Comput. Electron. Agr. **74**: 176-194, 2010.

Rustioni L., Basilico R., Fiori S. *et al*.: Grape colour phenotyping: development of a method based on the reflectance spectrum. – Phytochem. Anal. **24**: 453-459, 2013.

Rustioni L., Rocchi L., Guffanti E. *et al*.: Characterization of Grape (*Vitis vinifera* L.) Berry Sunburn Symptoms by Reflectance. – J. Agric. Food Chem., DOI: 10.1021/jf405772f, 2014.

Steele M.R., Gitelson A.A., Rundquist D.C., Merzlyak M.N.: Nondestructive estimation of anthocyanin content in grapevine leaves. – Am. J. Enol. Viticult. **60**: 87-92, 2009.

Tian Q., Giusti M.M., Stoner G.D.: Screening for anthocyanins using high-performance liquid chromatography coupled to electrospray ionization tandem mass spectrometry with precursor-ion analysis, product-ion analysis, common-neutral-loss analysis, and selected reaction monitoring. – J. Chromatogr. A **1091**: 72-82, 2005.

Tremblay N., Wang Z., Cerovic Z.G.: Sensing crop nitrogen status with fluorescence indicators. A review. – Agron. Sustain. Dev. **32**: 451-464, 2012

Valeur B., Berberan-Santos M.: Molecular Fluorescence - Principles and Applications. 2nd ed. Pp. 592. Wiley-VCH, Weinheim, 2012

Zhang H., Lan Y., Suh C.P.-C. *et al*.: Fusion of remotely sensed data from airborne and ground-based sensors to enhance detection of cotton plants. – Comput. Electron. Agr. **93**: 55-59, 2013.